and the dashed lines represent the prediction from eq 1 for four-arm and eight-arm stars, respectively, using the same values of the constants. The diffusion coefficients for the four- and eight-arm stars are much greater than predicted by the $f - 2$ dependence in the exponential of eq 1. For example, the predicted value of D^* for the four-arm star with $M_a = 40\,000$ is 2.5×10^{-17} cm^2/s, while the measured value is 5×10^{-14} cm^2/s. The comparison of D^*'s for the eight-arm star with $M_a = 60\,000$ is even worse, 1.4×10^{-39} cm^2/s predicted versus 2×10^{-15} cm^2/s measured. In contrast, the tracer diffusion coefficients of all the star molecules in microgels are described approximately by a single-exponential law, which is independent of the number of arms on the star. We conclude from this result that diffusion of a star-branched molecule by arm retraction does not require simultaneous retraction of more than one arm. Diffusive steps may occur by retraction of one arm at a time.

While we have been able to rule out very large differences in the diffusion coefficient as a function of f, it is expected that a weaker dependence must remain. An intuitive understanding can be gained by assuming that individual arm retractions are uncorrleated and that the branch point moves a distance proportional to $1/f$ each time a single arm retracts. This assumption leads directly to a diffusion coefficient which scales as $1/f$. A detailed model which gives a similar result has been proposed by Rubinstein.[17] This relatively weak dependence is certainly within the range of uncertainty of our data.

Acknowledgment. The financial support of this research to E. J. Kramer by the NSF-DMR Polymers Program under Grant DMR-8303174 is gratefully acknowledged. K. R. Shull received partial support in the form of a ATT Ph.D. Fellowship. We also benefited from the use of the facilities of the Cornell Materials Science Center, which is funded by the DMR-MRL program of the NSF. We greatly appreciate the help of Dr. Peter Mills, whose previous measurements of the diffusion of four- and eight-arm stars led to the experiments described here. We especially thank J. W. Mayer for his encouragement and helpful discussions on all aspects of forward recoil spectrometry and D. S. Pearson, W. W. Graessley, and E. Helfand for useful discussions.

Registry No. PS, 9003-53-6.

References and Notes

(1) Doi, M.; Edwards, S. F. *J. Chem. Soc., Faraday Trans. 2* **1978**, *74*, 1789.
(2) Doi, M.; Edwards, S. F. *J. Chem. Soc., Faraday Trans. 2* **1978**, *74*, 1802.
(3) Doi, M.; Edwards, S. F. *J. Chem. Soc., Faraday Trans. 2* **1978**, *74*, 1818.
(4) deGennes, P.-G. *J. Phys.* **1975**, *36*, 1199.
(5) Graessley, W. W.; Roovers, J. *Macromolecules* **1979**, *12*, 959.
(6) Pearson, D. S.; Helfand, E. *Macromolecules* **1984**, *17*, 888.
(7) Klein, J. *Macromolecules* **1986**, *19*, 105.
(8) Graessley, W. W. *Adv. Polym. Sci.* **1982**, *47*, 67.
(9) Klein, J.; Fletcher, D.; Fetters, L. J. *Nature (London)* **1983**, *304*, 526.
(10) Antonietti, M.; Sillescu, H. *Macromolecules* **1986**, *19*, 798.
(11) Green, P. F.; Mills, P. J.; Palmstrøm, C. J.; Mayer, J. W.; Kramer, E. J. *Phys. Rev. Lett.* **1984**, *53*, 2145.
(12) Mills, P. J.; Green, P. F.; Palmstrøm, C. J.; Mayer, J. W.; Kramer, E. J. *Appl. Phys. Lett.* **1984**, *45*, 957.
(13) Green, P. F.; Mills, P. J.; Kramer, E. J. *Polymer* **1986**, *27*, 1063.
(14) Green, P. F. Ph.D. Thesis, Cornell University, 1985.
(15) Antonietti, M.; Coutandin, J.; Sillescu, H. *Macromolecules* **1986**, *19*, 793.
(16) Bartels, C. R.; Crist, B.; Fetters, L. J.; Graessley, W. W. *Macromolecules* **1986**, *19*, 785.
(17) Rubinstein, M. *Phys. Rev. Lett.* **1986**, *57*, 3023.

Mutual Diffusion in the Miscible Polymer Blend Polystyrene/Poly(xylenyl ether)

Russell J. Composto* and Edward J. Kramer

Department of Materials Science and Engineering and the Materials Science Center, Bard Hall, Cornell University, Ithaca, New York 14853

Dwain M. White

General Electric Corporate Research and Development, Schenectady, New York 12301.

Received November 19, 1987; Revised Manuscript Received February 18, 1988

ABSTRACT: We have used forward recoil spectrometry to measure the mutual diffusion and tracer diffusion coefficients, D and D^*, in the miscible polymer blend of deuteriated polystyrene (d-PS)/poly(xylenyl ether) (PXE) containing a volume fraction $\phi = 0.55$ of d-PS. In this blend, D^* of the faster diffusing PS molecules of degree of polymerization N_{PS} decreases as N_{PS}^{-2} as expected from reptation. On the other hand D decreases as N_{PS}^{-1}, an observation in strong support of the "fast theory" of mutual diffusion which predicts that D is controlled by the D^* of the faster moving species, i.e., $D = 2\phi(1 - \phi)D_T(\chi_S - \chi)$, where χ and χ_S are the Flory interaction parameter of the blend and its value at the spinodal and D_T is the transport coefficient given by $D_T = (1 - \phi)D^*_{PS}N_{PS} + \phi D^*_{PXE}N_{PXE}$. While at low temperatures (e.g., 200 °C), D is much larger than D^*, the difference between D and D^* diminishes with increasing temperature until finally at the highest temperatures (e.g., 310 °C) D is less than D^*. This change in the relative values of D and D^* is due to the temperature dependence of χ. Using the measured values of D^* and D, we find that $\chi(T) = 0.112 - (62/T)$. The D and D^*'s were also measured as a function of composition in d-PS/PXE blends ranging from $\phi = 0.0$ to $\phi = 1.0$ at a temperature 66 °C above the glass transition temperature of each blend. Under these conditions D is much larger than the D^*'s, an increase predicted quantitatively by the "fast theory" using the same $\chi(T)$ determined for the $\phi = 0.55$ blend.

Introduction

Mutual diffusion or interdiffusion in miscible polymer blends, aside from its practical importance in the control of phase separation and homogenization, is of great interest for testing the relationship between the thermodynamics of such blends and their diffusion behavior.[1-13] de Gennes[14] was the first to point out that because the combinatorial entropy of mixing of polymers is so small, scaling as N^{-1}

0024-9297/88/2221-2580$01.50/0

where N is the degree of polymerization, the mutual diffusion of chemically dissimilar polymers will be dominated by the excess enthalpy and entropy of segment–segment mixing. In the usual mean-field approximation, the excess Gibbs free energy of mixing per segment can be represented by a regular solution model,[15] so that

$$\Delta G_{\mathrm{mix}}^{\mathrm{ex}} = \chi \phi_A \phi_B k_B T \tag{1}$$

where k_B, T, ϕ_A, and ϕ_B are the Boltzmann constant, absolute temperature, and volume fractions of the components A and B in the binary blend, respectively. The strength of the segment–segment interaction is represented by the Flory–Huggins interaction parameter χ. Within this approximation the mutual diffusion coefficient D is given by[2-6]

$$D = 2(\chi_s - \chi)\phi_A \phi_B D_T \tag{2}$$

where $\phi_A \phi_B D_T$ is an Onsager transport coefficient and χ_s is the interaction parameter at the spinodal

$$\chi_s = \frac{1}{2}\left[\frac{1}{\phi_A N_A} + \frac{1}{\phi_B N_B}\right] \tag{3}$$

where N_A and N_B are the degrees of polymerization of the polymer components represented by the subscripts.

Before presenting the current theories which predict D_T of a binary blend from the individual mobilities of its components, it is necessary to accurately define what is meant by tracer diffusion, self-diffusion, and mutual diffusion.[16,17] In tracer experiments, the tracer diffusion coefficient D^* of a dilute concentration of labeled A or B chains is measured in a matrix blend of A and B chains which may differ in length and chemical species from the labeled ones. Self-diffusion, on the other hand, is simply a special case of tracer diffusion. Here, the diffusing chains and the matrix chains must be chemically identical, except for the label, and of the same degree of polymerization. The most crucial characteristic of tracer diffusion, as far as this paper is concerned, is that the driving force for tracer diffusion is dominated by the combinatorial entropy of mixing (i.e., $\Delta G_{\mathrm{mix}}^{\mathrm{ex}} \approx 0$).

While most experiments have measured the diffusion of a dilute polymeric species because the tracer diffusion coefficient thus obtained is easy to interpret theoretically,[18] most diffusion problems of practical interest involve concentrated diffusion couples. Consider a binary diffusion couple of an A/B blend which contains volume fractions ϕ_1 and ϕ_2 of the A component on either side of an interface. In their seminal paper, Brochard, Jouffroy, and Levinson,[2] hereafter abbreviated as BJL, make the assumption that the diffusion fluxes of the segments of A and B chains are equal and opposite across the interface. This assumption requires a gradient in pressure ∇P across the couple and leads to an expression for D_T given by

$$\frac{1}{D_T} = \frac{\phi_B}{D^*_A N_A} + \frac{\phi_A}{D^*_B N_B} \tag{4}$$

An identical expression was derived independently by Binder.[3] Note that in this case the mutual diffusion coefficient will be controlled by the diffusion of the slower moving component if the mobilities of the two components are very different. Several experiments seem to support this "slow theory".[11,13]

While the total fluxes of A and B segments across the interface must be equal, it is well-known from diffusion experiments in solids that such fluxes do not have to be wholly diffusive.[16,17] The two diffusion fluxes, $\mathbf{J}_A$ and $\mathbf{J}_B$, may differ and a bulk (or convective) flow of the blend as a whole may occur to compensate. (In this case *both A and B* segments move with a velocity $\mathbf{V}$ toward the side of the diffusion couple with the higher concentration of the faster diffusing species (say A), such that, $\mathbf{J}_A + \mathbf{V}\phi_A/\Omega = -\mathbf{J}_B + \mathbf{V}\phi_B/\Omega$, where Ω is the volume of one quasi-lattice cell.) One can imagine that the bulk flow velocity is a response to the pressure gradient of BJL which reduces that pressure gradient nearly to zero if the mechanisms for flow are fast enough. While Kramer et al.[4] invoke a certain mechanism (vacancy flux) for this bulk flow, it was also pointed out that any mechanism which will prevent the build up of the pressure gradient will give the same result. Using a more general approach similar to the one sketched above, Sillescu[5,6] eliminates any gradient in pressure by invoking the Gibbs–Duhem equation. Although the Kramer et al. and Sillescu theories appear different, both define the mutual diffusion coefficient for a system where unequal diffusion fluxes are compensated by a bulk flow in the diffusion couple. Thus, both theories yield the same expression for D_T

$$D_T = \phi_B D^*_A N_A + \phi_A D^*_B N_B \tag{5}$$

A more recent theory of Brochard derives a bulk flow velocity from irreversible thermodynamics.[21] This new theory also arrives at the "fast" theory result, eq 5. Note that while the "slow theory" predicts a D which is controlled by the diffusion of the slower moving component, the "fast theory" (i.e., eq 5) says it is controlled by diffusion of the faster moving one. Green et al.[19] performed marker displacement experiments in which inert markers were placed at the initial interface between a thick film of long PS chains and a thick film of short PS chains. These results showed that a bulk flow occurred ($\mathbf{V} \neq 0$) during interdiffusion of the polymers in agreement with the "fast theory".

In order to explain the marker results, Brochard and de Gennes[20] have revised the earlier "slow theory" by proposing a hybrid, "fast–slow theory". They claim that for a characteristic diffusion distance less than

$$l = (D^*_A \tau_B)^{1/2} = \langle R_B^2 \rangle^{1/2} \left(\frac{D^*_A}{3\pi^2 D^*_B}\right)^{1/2} \tag{6}$$

the slower moving B macromolecules are swollen like a gel by the faster moving A ones so that the "fast theory" holds, whereas for greater diffusion distances a pressure gradient develops so that the "slow theory" result obtains. Note that this swelling is analogous to the bulk flow flux in the "fast theory". In eq 6, τ_B is the reptation time and $\langle R_B^2 \rangle^{1/2}$ is the root-mean-square end-to-end distance of the B chains. This idea seemed to explain the results of the marker displacement experiments in which the slower B molecules were extremely long ($M_{w,PS} = 20\,000\,000$), since the l's, which ranged from 1 to 20 μm, were larger than the diffusion distances that could be probed by the ion beam technique used. (However, it is possible to criticize the consistency of a theory which invokes a mechanism (reptation) for the onset of the pressure gradient that is also a mechanism for viscous flow and hence for the relaxation of such pressure gradients.)

Now that a relationship between the transport coefficient D_T in a polymer blend and the D^*'s of its components has been presented, one can use this relationship in order to extract the Flory–Huggins parameter χ from the measured values of D and the D^*'s. Upon rewriting eq 2, χ is given by

$$\chi = \chi_S - \frac{D}{2\phi_A \phi_B D_T} \tag{7}$$

Table I
Weight-Average Degrees of Polymerization and Polydispersity Indices of the Various Polystyrene and Poly(xylenyl ether) Polymers Together with Their Sources

N_{PS}	N_{PXE}	polydispersity index	source
		Deuteriated PS and PXE	
529		1.06	Polymer Laboratories
1058		1.1	Polymer Laboratories
2452		1.1	Polymer Laboratories
5000		1.1	Polymer Laboratories
7885		1.3	Polymer Laboratories
	225	1.9	General Electric
	383	2.4	General Electric
		Protonated PS and PXE	
529		1.06	Pressure Chemical
865		1.06	Pressure Chemical
2452		1.06	Pressure Chemical
3750		1.06	Pressure Chemical
19230		1.2	Pressure Chemical
	292	2.3	General Electric

In order for high N polymers to be miscible, χ normally must be negative and consequently the second term should dominate eq 7.[22] However, for a blend which exhibits a lower critical solution temperature, χ should become less negative with increasing temperature until, finally, χ becomes greater than χ_S. Since χ strongly influences the diffusion in concentrated couples, one should witness a corresponding decrease in the value of D, compared with its D^*'s, as temperature increases. These predictions will be tested quantitatively.

In two previous short papers[1,7] we outlined results which demonstrated that the mutual diffusion of deuteriated polystyrene (d-PS) chains and protonated poly(xylenyl ether) (PXE) chains was significantly enhanced by the strong attractive interaction between them and that the faster moving component (d-PS) in the blend dominates the measured mutual diffusion coefficient. In this paper we complete the experimental proof that the "fast theory" describes mutual diffusion in this polymer blend and then use measurements of D and D^* as a function of temperature to extract the temperature dependence of $\chi(T)$. Using these values for $\chi(T)$, we reexamine the composition dependence of the mutual diffusion coefficient $D(\phi)$ for d-PS/PXE blends ranging from pure d-PS to pure PXE.

Experimental Methods

To measure the tracer diffusion coefficient in blends of polystyrene (PS) and poly(xylenyl ether) (PXE), diffusion couples were made which consisted of a thin (~20 nm) deuteriated polystyrene film (d-PS) or deuteriated poly(xylenyl ether) (d-PXE) film on top of a thick (~2 μm) film of a blend of protonated PS and PXE, which served as the matrix into which the diffusion was carried out. The matrix film was prepared by pulling a 2 cm × 2 cm silicon wafer, at a constant rate, from a blend of PS/PXE dissolved in chloroform. The film of the deuteriated tracer polymer was prepared from a chloroform solution of d-PS or d-PXE polymer by spin casting on a glass substrate. The deuteriated film was floated off onto the surface of a water bath and then picked up with the PS/PXE coated wafer. The tracer diffusion couples used in this study are shown in Figure 1a where ϕ is the volume fraction of PS in the matrix and N represents the weight-average degree of polymerization of the d-PS or d-PXE chains. The weight-average degree of polymerization (N), polydispersity index, and source of the deuteriated and protonated polymers used in this study are shown in Table I.

Whereas the tracer couples were constructed so as to follow the diffusion of a dilute amount of labeled chains, mutual diffusion experiments are concerned with the diffusion of both species in a binary diffusion couple. The mutual diffusion couple was formed by spin casting a base film (~2 μm thick) of d-PS/PXE on a silicon-wafer substrate from a solution containing a volume fraction ϕ_1 of d-PS in chloroform. A second film (~350 nm) was prepared from another solution of different composition, ϕ_2, by spin casting on a glass substrate. After drying, this film was floated off onto a surface of a water bath from where it was picked up with the d-PS(ϕ_1)/PXE coated wafer to produce a bilayer-film diffusion couple. The initial profile between the two blends is shown schematically in the lower portion of Figure 1b.

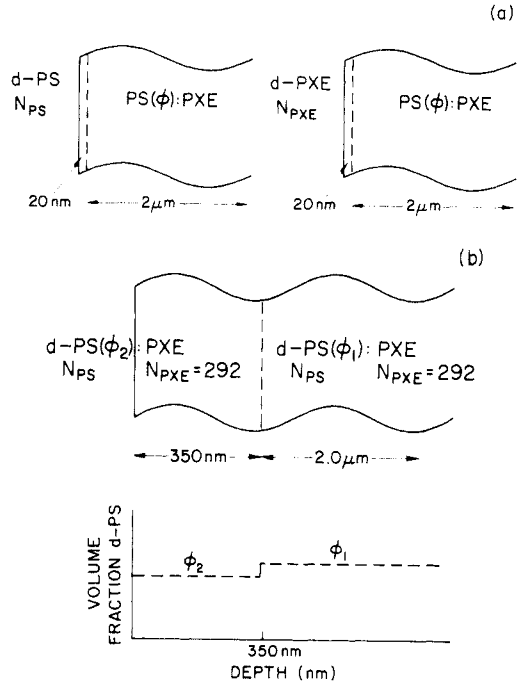

Figure 1. (a) Tracer diffusion couple consisting of a thin deuteriated film of d-PS or d-PXE on a thick protonated PS/PXE blend containing a volume fraction ϕ of PS. The weight-average degree of polymerization is denoted by N_{PS} and N_{PXE} for d-PS and d-PXE, respectively. (b) Mutual diffusion couple consisting of two films of d-PS/PXE containing weight-average degrees of polymerization of N_{PS} and 292 for d-PS and PXE, respectively. The top film has a volume fraction ϕ_2 of d-PS while the bottom film has a volume fraction ϕ_1. The lower diagram shows the initial step (~10%) in the volume fraction versus depth profile of a typical couple.

Both the tracer and mutual diffusion couples at a given volume fraction ϕ were heated simultaneously to a temperature T under vacuum (<10^{-6} Torr) for a given diffusion time t. After annealing, the concentration versus depth profile of d-PS or d-PXE in the film was measured by forward recoil spectrometry (FRES). In this technique, a beam of doubly ionized helium $^4He^{2+}$ ions with an energy E_0 = 2.8 MeV strikes the diffusion couple at a glancing angle of 15°. An energy-sensitive detector records the number and energy of the deuterium nuclei (^2H) and hydrogen nuclei (^1H) which enter the detector. Since the ^2H nuclei recoiling from the surface receive a much higher fraction (~2/3) of E_0 than do ^1H nuclei (~1/2), the surface peaks due to ^2H and ^1H are well separated in energy. For a scattering nucleus which lies at a depth x below the surface, the He^{2+} ions will lose energy via electronic excitations before the recoil collision and then the scattered nucleus will also lose energy as it traverses the film on its outward path. Therefore ^2H and ^1H recoiling from depths below the surface are shifted to lower energies than the ^2H and ^1H recoiling from the surface. The number of nuclei that recoil from a particular depth within the sample is proportional to the concentration of ^2H or ^1H at that depth. Figure 2 shows a typical FRES spectrum for the tracer diffusion of d-PS chains into a protonated PS/PXE matrix. Note that the energies of ^2H nuclei recoiling from deep in the polymer (≥750 nm) will overlap in energy with the surface ^1H nuclei. Therefore the optimal characteristic diffusion distance w for tracer diffusion corresponds to about 330 nm while the optimal thickness for the top film in a mutual diffusion couple is about 350 nm. The forward recoil spectrum can be analyzed quite easily to obtain the depth profile of d-PS or d-PXE chains in the matrix. Details of this ion beam analysis technique have been published elsewhere.[23-26]

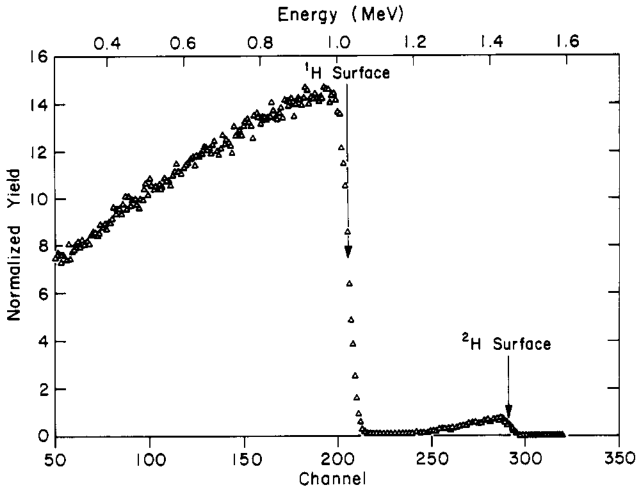

Figure 2. FRES spectrum from a sample of a thin film of d-PS (weight-average molecular weight = 255 000) which has diffused into a thick film PS/PXE matrix for 2 × 10^4 s at 206 °C. The volume fraction of PS in the matrix is 0.55 and the molecular weights of the PS and PXE in the matrix are 255 000 and 35 000, respectively.

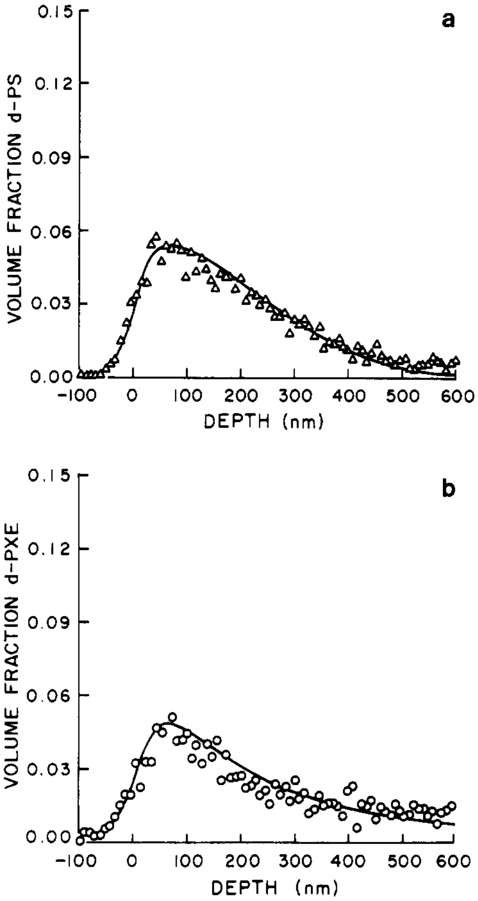

Figure 3. Volume fraction versus depth profiles corresponding to (a) d-PS (from the FRES spectrum in Figure 2) and (b) d-PXE (weight-average molecular weight 46 000) diffused in the same PS:PXE blend as (a) for 1.56 × 10^5 s at 206 °C. The solid lines were theoretical fits using $D_{PS}^* = 1.2 \times 10^{-14}$ and $D_{PXE}^* = 2.2 \times 10^{-15}$ cm^2/s for d-PS and d-PXE, respectively.

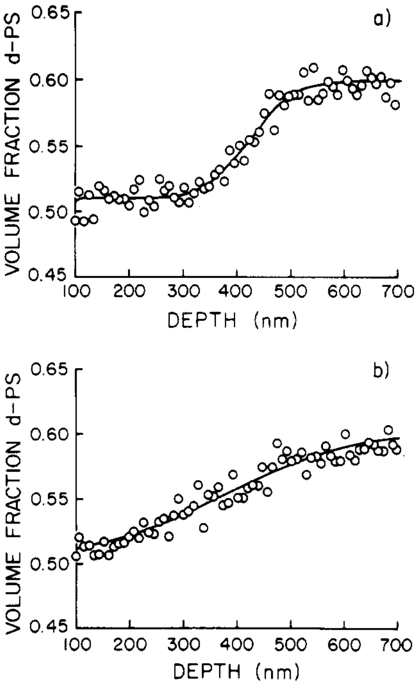

Figure 4. Volume fraction of deuteriated polystyrene in a d-PS(N_{PS} = 2452)/PXE(N_{PXE} = 292) mutual diffusion couple, (a) as deposited and (b) after diffusion for 1800 s at 206 °C. The solid lines represent a best fit of eq 9 to the data by using an instrumental resolution of 80 nm (a) and a D of 1.1 × 10^{-13} cm^2/s (b).

Figure 3 shows the depth profile for d-PS (a) and d-PXE (b) tracer films diffused into protonated PS/PXE blends which contained 0.55 volume fraction of PS. Since the d-PS and d-PXE from the thin layer becomes rapidly diluted, the combinatorial entropy of mixing is the only driving force for diffusion over most of the diffusion time. Thus, the volume fraction profile can be described by the tracer, or infinite dilution, diffusion coefficient D^*. The depth profile for monodisperse chains diffusing in a semiinfinite matrix is given by the solution to Fick's second law[17]

$$\varphi(x) = \frac{1}{2}\left[\operatorname{erf}\left(\frac{(h-x)}{w}\right) + \operatorname{erf}\left(\frac{(h+x)}{w}\right)\right] \qquad (8)$$

where h, the initial thickness of the tracer film, is found by integrating the experimental depth profile and w is the characteristic diffusion distance, $2(D^*t)^{1/2}$. A theoretical volume fraction profile can be computed by convoluting $\varphi(x)$ from eq 8 with the instrumental resolution function, a Gaussian with a full width at half-maximum of 80 nm. The tracer diffusion coefficient is varied until a good fit of the theoretical profile to the experimental profile is achieved. The solid line in Figure 3a represents the best fit to the data using $D^*_{PS} = 1.2 \times 10^{-14}$ cm^2/s. The tracer diffusion coefficient of the polydisperse d-PXE chains was found by modifying eq 8 to include polydispersity effects.[27] The solid line in Figure 3b represents this polydisperse fit to the data by using $D^*_{PXE} = 2.2 \times 10^{-15}$ cm^2/s for chains of weight-average degree of polymerization 383.

Because of a strong concentration dependence of the glass transition temperature T_g of most polymer blends, mutual diffusion coefficients are not easily measured.[1,7-13,27] For example, the glass transition temperature of PS/PXE blends is T_g(°C) = 215.4–173.8ϕ_{PS} + 75.1ϕ_{PS}^2 – 11.8ϕ_{PS}^3 from differential scanning calorimetry.[27] Consider the diffusion profile for a diffusion couple consisting of pure PS and pure PXE which is heated to temperature T. Because of the drastic difference between the glass transition temperatures of PS (105 °C) and PXE (216 °C for N_{PXE} = 292) and mobilities of PS and PXE, the resulting concentration profile cannot be described by a simple, concentration-independent, diffusion coefficient (i.e., eq 8). Since D varies continuously along the interface of this couple, it is quite difficult to extract values of D.[27] However, if the diffusion couple consists of two d-PS/PXE blends which differ by 10% in concentration, a single mutual diffusion coefficient associated with the average composition at the interface of the couple can be measured. Figure 4 shows the volume fraction profile of d-PS versus depth x for a mutual diffusion couple before (a) and after (b) diffusion. The initial ϕ_1 of the bottom film is 0.60 while that of the top film is 0.51. The interface between the two films in the experimental profile of the undiffused sample appears somewhat diffuse as a

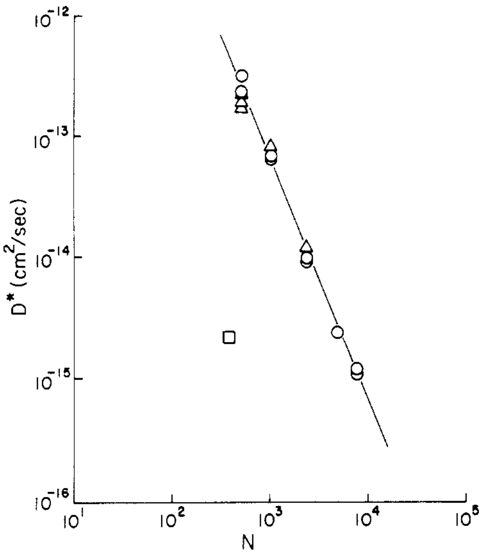

Figure 5. Tracer diffusion coefficients D^* of d-PS (circles, triangles) and d-PXE (square) as a function of the weight-average degrees of polymerization N of the d-polymers. The diffusion was at 206 °C into a blend matrix of 0.55 volume fraction PS (N_{PS}) and PXE (N_{PXE} = 292). The circles and squares correspond to a matrix N_{PS} of 19 230, while the triangles correspond to a matrix N_{PS} which is about equal to the N_{PS} of the d-PS. The solid line is a line of slope −2 as predicted by reptation.

result of the limited instrumental resolution mentioned previously. The solid line in Figure 4a corresponds to a step function convoluted with the instrumental resolution function. After diffusion, however, the interface becomes significantly broadened as shown in Figure 4b. Since the composition of the couple varies by only 0.09, the mutual diffusion coefficient D can be assumed to be constant over this range. The depth profile should be given by the Fickian solution[1,7,8,17]

$$\varphi(x) = \frac{1}{2}(\phi_2 - \phi_1)\left[\operatorname{erf}\left(\frac{(h+x)}{w}\right) + \operatorname{erf}\left(\frac{(h+x)}{w}\right)\right] + \phi_1 \tag{9}$$

where h is the thickness of the top film and $w = 2(Dt)^{1/2}$. The solid line in Figure 4b represents the best fit of eq 9 to the data. This fit requires a D of 1.1×10^{-13} cm²/s which we take as the value at the interfacial composition, i.e., ϕ = 0.555.

Results

Molecular Weight Dependence. To provide a critical test for the "fast" and "slow" theories, we measured both the tracer diffusion coefficients D^* and mutual diffusion coefficients D in a PS/PXE blend containing 0.55 volume fraction PS. The D^*'s of d-PS (circles) and d-PXE (squares) are plotted in Figure 5 as a function of N, the degree of polymerization of the tracer polymer. The triangles will be discussed below. The weight-average degree of polymerizations of the protonated PXE and PS in the ϕ = 0.55 blend matrix were 292 and 19 230, respectively. All samples were heated to 206 °C, a temperature 66 °C above the T_g of this blend, to carry out diffusion. Note that D^* of d-PS scales as N^{-2} as predicted by reptation. Note also that D^* of PXE is nearly 2 orders of magnitude smaller than D^* of PS at the same value of N.

In the mutual diffusion experiments to be discussed below, the relevant D^*'s for PS were for d-PS chains diffusing into a blend of PS/PXE where the degree of polymerization of the PS in the matrix matches that of the d-PS tracer. Such D^* measurements were also carried out and the results are shown as the triangles in Figure 5. As expected for reptation, the D^*'s do not depend on the degree of polymerization of PS in the matrix as long as this degree of polymerization equals or exceeds that of the d-PS tracer. Similar experiments were conducted to ensure that the D^* of the lower degree of polymerization PXE was not seriously increased by decreasing the degree of polymerization of polystyrene.

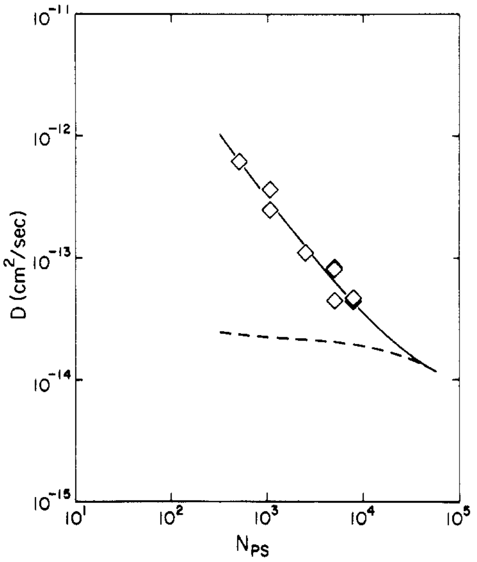

Figure 6. Mutual diffusion coefficient D in the d-PS/PXE blend system at 206 °C and a 0.55 volume fraction of d-PS as a function of the degree of polymerization N_{PS} of d-PS; N_{PXE} of the PXE is 292 for all samples. The solid line is the prediction of the fast theory whereas the dashed line is the prediction of the slow theory.

As shown in Figure 6, the value of the mutual diffusion coefficient D increased as the degree of polymerization N_{PS} of the d-PS chains decreased, scaling approximately as N_{PS}^{-1}. The mutual diffusion couples were heated to the same temperature as the tracer diffusion couples, 206 °C. The weight-average degree of polymerization of the PXE was held constant at 292 for all mutual diffusion couples. Since PS was the faster moving species in these blends the observed variation of D with N_{PS} constitutes strong qualitative support for the "fast theory".

Temperature Dependence. The temperature dependence of the tracer diffusion coefficients D^* and mutual diffusion coefficient D was measured for PS/PXE blends containing 0.55 volume fraction PS. In the tracer experiments, the weight-average degrees of polymerization N for d-PS and d-PXE were 2452 and 292, respectively, while N's for the matrix chains in the tracer couples were 3750 and 292 for PS and PXE, respectively.[28] For temperatures not too much greater than the glass transition temperature, the temperature dependence of D^*/T has been shown to be described quite well by a form of the Vogel–Fulcher equation,[29]

$$\log\left(\frac{D^* T_{\mathrm{ref}}}{T}\right) = A' - \frac{B}{(T - T_\infty)} \tag{10}$$

where A', B, and T_∞ are empirical parameters and where T_{ref} is a reference temperature. The derivation of eq 10 is presented in the Appendix. As shown in Figure 7, the tracer diffusion coefficients for d-PS (circles) and d-PXE (squares) increased rapidly as the diffusion temperatures increased from 180 to 310 °C. The dashed lines are nonlinear least-square fits of eq 10 to the experimental D^*'s where the empirical parameters B_{PS} = 601, B_{PXE} = 555, and T_∞ = 361 K were obtained at reference temperature of 500 K. Except at the lowest T, the temperature dependence of the D^*'s for d-PS and d-PXE diffusing in a ϕ = 0.55 blend are in good agreement with eq 10. Note that both D^*_{PS} and D^*_{PXE} increase at about the same rate with increasing temperature (i.e., both D^*_{PS} and D^*_{PXE} can

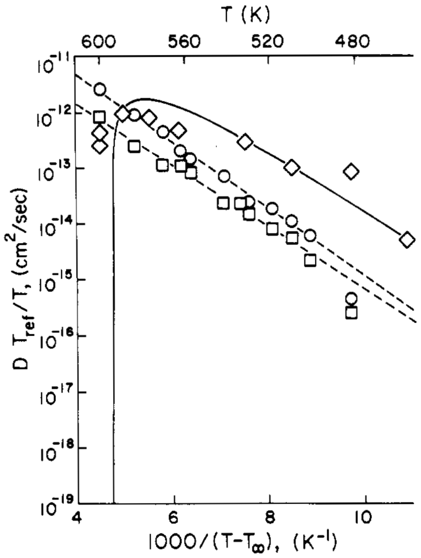

Figure 7. Temperature dependence of the tracer diffusion coefficients of d-PS (circles) and d-PXE (squares) of weight-average degrees of polymerization 2452 and 292, respectively, and the mutual diffusion coefficients (diamonds) of d-PS/PXE blends of weight-average degrees of polymerizations 2452 and 292, respectively. The values used for T_{ref} and T_∞ were 500 and 361 K, respectively. The matrix films for the tracer experiments were a PS/PXE blend containing 0.55 volume fraction PS while the average volume fraction of d-PS in the mutual diffusion couple was also 0.55.

be described by using B's that are nearly the same).

Also shown in Figure 7 are the values of the mutual diffusion coefficients D (diamonds) for d-PS/PXE blends measured for a 0.55 volume fraction d-PS blend. The weight-average degree of polymerizations of the d-PS (N_{PS} = 2 452) and PXE (N_{PXE} = 292) were the same as those of the tracer molecules used to measure the D^*'s. Note that at low temperatures D is almost an order of magnitude greater than the D^*'s of the components of the blend. Qualitatively, this enhancement can be attributed to the existence of segment-interaction-enhanced mutual diffusion first predicted by de Gennes.[14] Note also that the temperature dependence of D deviates from that of the D^*'s such that the difference between D and the D^*'s gradually diminishes with increasing temperature until finally D becomes somewhat less than the D^*'s at 310 °C. As discussed below this decrease in D can be attributed to the temperature dependence of the interaction parameter χ.

Composition Dependence. The tracer diffusion coefficients D^* and mutual diffusion coefficient D were also measured as a function of the volume fraction ϕ of PS in PS/PXE blends ranging from ϕ = 1.0 (pure PS) to ϕ = 0.0 (pure PXE). The values of D^* are plotted in Figure 8 for d-PS (N_{PS} = 2452) and d-PXE (N_{PXE} = 292).[28] To partially compensate for the decreasing glass transition temperature T_g of the blend with increasing ϕ, the diffusion temperature T was adjusted so that $T - T_g$ was held constant at 66 °C. The weight-average degrees of polymerization of the matrix PS and PXE components were 3750 and 292, respectively. As shown in Figure 8, the D^*'s depended differently on blend composition, with D^*_{PS} surprisingly exhibiting a strong minimum with ϕ, whereas D^*_{PXE} was at first constant and then increased monotonically as ϕ approached 1.0. Note also that D^* for the 292 PXE component was about a factor of 80 lower than D^* for the 2452 d-PS component at the lower ϕ's.

Values of the mutual diffusion coefficient are also plotted as a function of composition in Figure 8. The weight-average degree of polymerization for the components in the d-PS/PXE blend were 2452 and 292 for d-PS and PXE, respectively. Note that at intermediate compositions D is almost an order of magnitude higher than either of the D^*'s of the components of the blend, again providing strong qualitative evidence for the existence of segment-interaction-enhanced mutual diffusion.

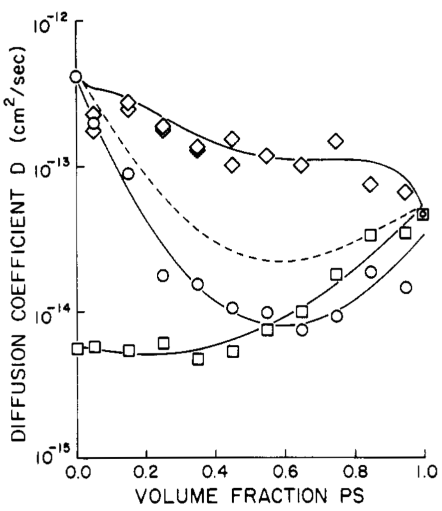

Figure 8. Diffusion coefficients versus composition in the PS/PXE system. The squares and circles represent the tracer diffusion coefficients D^* of d-PXE (N_{PXE} = 292) and d-PS (N_{PS} = 2452) in blends of PS/PXE. The diamonds represent the measured mutual diffusion coefficients in the d-PS/PXE diffusion couples. The lower solid lines represent smoothed values of $D^*_{d\text{-}PXE}$ and $D^*_{d\text{-}PS}$ used in the calculation for D. The upper solid line and dashed line represent the D predicted by eq 2 and 5 with, and without, segment–segment interaction enhancement, i.e., for $\chi = 0.112 - [62/T(\mathrm{K})]$ and $\chi = 0.0$, respectively.

Discussion

The predictions of both the "slow" and "fast" theories of the mutual diffusion coefficient D will be compared quantitatively with the experimental values, using the measured values of the tracer diffusion coefficients, D^*_{PS} and D^*_{PXE}. In computing D, χ_S is set equal to its mean-field value given by eq 3.[30] Since $|\chi| \gg \chi_S$ for a diffusion temperature of 206 °C, the $(\chi_S - \chi)$ term in eq 2 is insensitive to N_{PS}. The solid line in Figure 6 shows the D computed by using the "fast theory" (eq 2 and 5) where a χ of −0.0178 produces the best-least-squares fit to the data. Utilizing the same χ, the dashed line shows the D computed from the "slow theory" (eq 2 and 4). Since the D predicted from the "slow theory" is dominated by the D^* of the slow PXE chains, whose N remains constant, a different choice of χ will only scale the dashed line up or down but can never produce a good fit to the measured D's. Clearly the data are in excellent agreement with the fast theory and in strong disagreement with the slow one. This comparison between theory and experiment demonstrates unequivocally that the mutual diffusion of a polymer blend is controlled by the diffusion of its faster moving species.

While it is clear that the fast theory describes the d-PS/PXE results well, the hybrid "fast–slow theory" of Brochard and de Gennes[20] might also. To demonstrate that this theory can be ruled out, we have computed from eq 6 the characteristic diffusion distance l beyond which the "slow theory" result should be observed. Unlike the long PS chains in the marker experiment by Green et al.[19] originally treated by Brochard and de Gennes, the slow moving PXE chains in our experiment are rather short and therefore the l's computed for these PS:PXE blends range from 11 to 39 nm, much smaller than the typical mutual

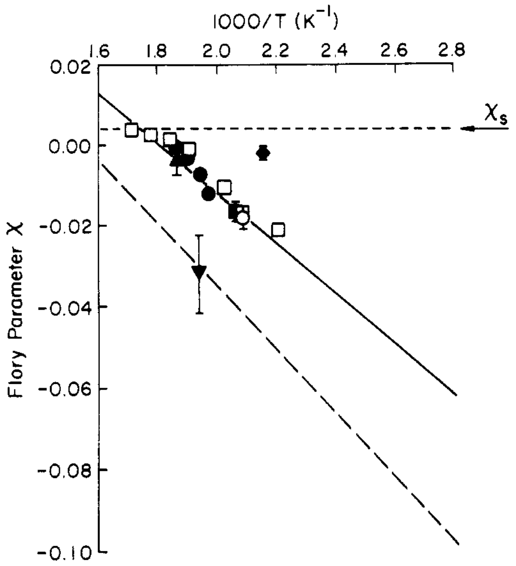

Figure 9. Temperature dependence of the segment–segment (Flory) interaction parameter, χ, in a d-PS/PXE blend containing 0.55 volume fraction of d-PS. The short-dashed line represents $\chi_S = 0.0039$ and the solid line $\chi = 0.112 - [62/T(\mathrm{K})]$. The open squares represent the χ's from D and D^* in Figure 7 while the open circle represents the average value of $\chi = -0.0178$ as computed from the diffusion data in Figure 6. The solid circles,[33] solid up-pointing triangle,[35] solid square,[36] and solid down-pointing triangle[34] represent χ's measured for dilute d-PS in PXE. The solid diamond[36] represents a χ measured for d-PS in a PS/PXE blends containing 0.50 volume fraction of PS plus d-PS. The temperatures for the SANS measurements (which were all made at room temperature where the blends are in the glassy state) correspond to estimates of the temperatures at which each blend fell out of equilibrium at the cooling rates given,[33-36] using the methods outlined in ref 37. The long-dashed line represents χ's measured at high temperatures by using SANS for dilute d-PXE in PS.[34]

diffusion distances of 200 nm measured by our FRES experiments. Thus, the Brochard and de Gennes theory predicts that the swelling of the PXE chains is negligible and that the slow theory should prevail, in strong disagreement with our results.

Knowing that the fast theory correctly describes the mutual diffusion process, we next demonstrate that the Flory–Huggins interaction parameter χ for the blend can be determined systematically from the measured values of $D(T)$ and $D^*(T)$. From eq 2 and 5, the interaction parameter is given by

$$\chi = \chi_S - \frac{D}{2\phi(1-\phi)[(1-\phi)D^*_{\mathrm{PS}}N_{\mathrm{PS}} + \phi D^*_{\mathrm{PXE}}N_{\mathrm{PXE}}]} \tag{11}$$

where D^*_{PS} and D^*_{PXE} are the tracer diffusion coefficients of PS and PXE, respectively. Values of the interaction parameter at various temperatures were extracted by using eq 11 and are plotted in Figure 9 for a $\phi = 0.55$ blend. The open squares correspond to χ's computed from the diffusion coefficients in Figure 7 while the open circle represents the average χ calculated from the diffusion coefficients given in Figure 6. Note that the χ's determined by our molecular weight and temperature experiments are consistent with each other. Our results show that χ becomes less negative (i.e., there is a less attractive segment interaction between d-PS and PXE) as T increases and that χ scales roughly as $1/T$. A least-squares fit to the data yields $\chi = 0.112 - 62/T$ (solid line). Also shown in Figure 9 is the interaction parameter at the spinodal, $\chi_S = 0.0039$, which was calculated by eq 3 with $N_{\mathrm{PS}} = 2452$ and $N_{\mathrm{PXE}} = 292$.[30]

Substituting $\chi(T) = 0.112 - 62/T$ and the D^*'s from Figure 7 into eq 2 and 5, the temperature dependence of the mutual diffusion coefficient D corresponding to a $\phi = 0.55$ blend can be predicted. This result, represented by a solid line in Figure 7, shows that at temperatures less than 280 °C, the predicted values of D agree quite well with the experimental values of D. Note that the retardation of D observed experimentally can be explained quite nicely by the temperature dependence of χ. As T increases, χ becomes more positive and therefore D becomes less and less enhanced by the excess enthalpy and entropy of mixing. Finally at high enough T, mutual diffusion becomes retarded rather than enhanced relative to tracer diffusion. Green and Doyle[31] observe a similar slowing down of D in the PS/d-PS system due to a small positive χ. Thus the thermodynamic "slowing down" at high T and the thermodynamic "speeding up" of D at low T show quite conclusively that the excess enthalpy of mixing strongly affects the interdiffusion process in PS/PXE blends.

Although from the simple Flory–Huggins model of the thermodynamics of polymer blends χ is expected to be independent of blend volume fraction ϕ, previous experiments on other blend systems have demonstrated that χ can change with composition.[32] Nevertheless the results of our mutual diffusion experiments show that the assumption of a composition-independent χ is reasonably good for the d-PS/PXE system. To demonstrate this point the mutual diffusion coefficient $D(\phi)$ was predicted by using eq 2 and 5 for the entire composition range ($0.0 \leq \phi \leq 1.0$) from the χ determined for the $\phi = 0.55$ blend. The predicted D's are shown as the solid line in Figure 8 and are in good agreement with the experimental data. Since these values of χ appear to predict the magnitude of $D(\phi)$ quite well, it appears that χ in the d-PS/PXE system is not a strong function of composition. The dashed line in Figure 8 represents the predicted D's expected if the mixing were ideal, i.e., $\chi = 0$. At extreme compositions, the difference between the predicted D (dashed line) expected for ideal mixing (i.e., $\chi = 0$) and the measured values of D is small, thus showing that mutual diffusion experiments are relatively insensitive to the composition dependence of $\chi(\phi)$ near $\phi = 0.0$ and 1.0. It is mainly at intermediate values of ϕ that one observes enhanced mutual diffusion due to a negative χ parameter.

One can also construct a phase diagram for a d-PS/PXE blend of degrees of polymerization $N_{\mathrm{PS}} = 2452$ and $N_{\mathrm{PXE}} = 292$. In the Flory–Huggins theory the free energy of mixing per quasi-lattice site for a d-PS/PXE mixture is given by[15]

$$\Delta G_{\mathrm{mix}} = k_{\mathrm{B}}T\left(\frac{\phi_{\mathrm{PS}}}{N_{\mathrm{PS}}}\ln\phi_{\mathrm{PS}} + \frac{\phi_{\mathrm{PXE}}}{N_{\mathrm{PXE}}}\ln\phi_{\mathrm{PXE}} + \chi(T)\phi_{\mathrm{PS}}\phi_{\mathrm{PXE}}\right) \tag{12}$$

where ϕ_{PS} and ϕ_{PXE} are the volume fractions of d-PS and PXE, respectively, and $\chi(T)$ is assumed to be composition independent and equal to the values we compute for a $\phi = 0.55$ blend. From eq 12, the phase diagram in Figure 10 was computed. The critical composition and temperature T_c are predicted to be $\phi = 0.27$ and 566 K, respectively. This value of T_c is consistent with the wide range of T_c's reported in the literature for various PS/PXE blends.[33,34]

It is worthwhile to compare the χ's measured by our mutual diffusion experiments using FRES with those found by small-angle neutron scattering SANS experiments for the PS/PXE system. In Figure 9 we compare our values of χ at $\phi = 0.55$ with those measured by Jelenic

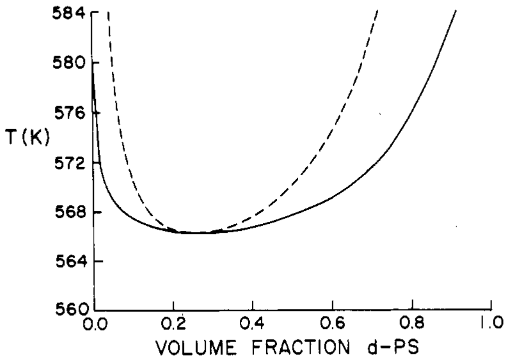

Figure 10. Calculated phase diagram for d-PS:PXE blends. The inner line represents the spinodal (- - -) and the outer the binodal (—). The degrees of polymerization were 2452 and 292 for d-PS and PXE, respectively.

et al.[33] (solid circles), Wignall et al.[35] (solid upward pointing triangle), and Maconnachie et al. (solid downward pointing triangle[34] and solid square[36]) measured χ for dilute d-PS in PXE. These experiments were carried out at room temperature where the blend is a glass; we have estimated, using the methods outlined in a separate publication,[37] the effective temperature at which equilibrium was established at the cooling rates inferred for these experiments and the measured D^*'s of PS. Note that our $\chi(T)$ (solid line) produces values that lie comfortably within the wide range of χ's found in the literature. Jelenic et al.[33] report an anomalous molecular weight dependence of χ where χ per unit volume ranges from -0.0124 to -0.0006 for d-PS of molecular weights of 25 000 to 465 000, respectively; this anomaly is largely eliminated by the estimation of the equilibration temperature; the higher molecular weight samples fall out of equilibrium at higher temperatures. Figure 9 also includes a value of χ for dilute d-PS in $\phi = 0.50$[36] (solid diamond) blends of PS/PXE. Since this experiment was also carried out at room temperature we have estimated the equilibration temperature using the same procedure[37] as for the data for d-PS in PXE.

In the only previous study concerning the temperature dependence of χ in the PS/PXE system, Maconnachie et al.[34] found that χ was described by $\chi(T) = 0.121 - 78/T$ (dashed line) for dilute d-PXE in PS. While these values of χ increase with increasing temperature at roughly the same rates as our results, the χ's measured by SANS are more negative than the χ's computed from the mutual diffusion experiments. As discussed below, this difference might be attributed to two possible causes, the first of which is deuterium labeling.

Yang et al.[38] show that deuteriation of the PS component in a PS/poly(vinyl methyl ether) (PVME) blend raises the lower critical solution temperature by about 40 °C. Since a similar increase in the upper critical solution temperature of d-PS/polybutadiene (PB) over PS/PB is also observed,[39] it appears that the interaction between a deuteriated component and its protonated partner is not the same as that between two protonated molecules. Thus, the values of χ measured in our studies are specific to the d-PS:PXE system and should not be assumed to hold true for the PS/d-PXE system or the PS/PXE system. Another possible reason for the difference between our results and Maconnachie et al.'s is the composition dependence of χ. In the SANS experiments, χ is measured for a dilute amount of d-PXE in a pure PS matrix while we compute the χ in a d-PS/PXE blend containing 0.55 volume fraction of d-PS. Using the SANS technique, Shibayama et al.[32] show that χ is a strong function of concentration in the d-PS/PVME system. Since these results were rationalized in terms of the different thermal expansion coefficients and thermal compressibilities in d-PS/PVME blends, some composition dependence of χ in the d-PS/PXE blends might also be expected.[40] Although, as shown in Figure 9, our composition studies of D suggest that the composition dependence of χ is weak, mutual diffusion experiments are relatively insensitive to χ at the extreme compositions (where the driving force for diffusion is mainly combinatorial entropy) and therefore we cannot rule out the composition dependence of χ in the dilute regime.

Recently several other groups have measured D in compatible blends in order to test the prevailing theories. Using infrared microdensitometry, Jordan et al.[41] studied the mutual diffusion in a polyethylene couple containing degrees of polymerization of N_A and of N_B, where 5% of the N_B molecules were deuteriated. They found that the broadening of the interface was controlled by the mobility of the faster moving (shorter) polymer chains in agreement with the fast theory. Since the interfacial broadening was roughly 500 μm, much greater than the characteristic distance l of ~ 1 μm, again the hybrid fast–slow theory predicts that the slow mode should dominate D, in disagreement with their experimental results.

In another study, Garabella and Wendorff[11] used small-angle X-ray scattering to indirectly measure the interdiffusion process between films of pure poly(vinylidene fluoride) PVDF and pure poly(methyl methacrylate) PMMA. However, several assumptions in the analysis procedure were made which weaken their claim that only the "slow theory" can explain their experimental results. The two most questionable assumptions were to estimate values of D^* and then to assume that these D^*'s were independent of composition (i.e., tracer diffusion coefficients of both components were not measured). Although they claim that their estimated D^* for PMMA agrees with the value found by Wu et al.,[12] this comparison should not be made because the diffusion coefficients measured by Wu et al. correspond to the intrinsic diffusion coefficients, not the tracer diffusion coefficients. Another questionable assumption was to ignore the composition dependence of the D^*'s. In their experimental setup, three different contributions to $D(\phi)$ were possible. Because pure films were used, the large variation in T_g ($\sim$140K) across the couple will produce a large change in both D^*'s with ϕ. Second, as shown by our data in Figure 8, even at constant $T - T_g$, an extra composition dependence of D^* can be produced by the compositional dependence of the monomeric friction coefficient ζ_0. A further complication might also be an enhancement of the D^* of the slower species due to constraint release.[27] All three of these effects have been shown to be quite important in the PS/PXE system. Thus although this is an interesting experiment, no conclusive judgements on the fast theory versus slow theory controversy should be drawn from it.

Using dynamic light scattering, Murschall et al.[13] claim that the mutual diffusion of unentangled poly(phenylmethylsiloxane) PPMS/PS blends follows the slow theory. This conclusion was based mainly on the similarity between the WLF parameters (i.e., C_1 and C_2) of the PPMS/PS blends and those of pure PS, the slower moving component. However, since Cohen[42] has shown that it is also possible to fit their data by using the C_1 and C_2 values of pure PPMS, these experiments cannot be used to accurately differentiate between the fast and slow theories.

Conclusions

1. In a miscible blend of d-PS/PXE containing 0.55 volume fraction of PS, the mutual diffusion coefficient D

increases as N_{PS}^{-1} with decreasing N_{PS}, where N_{PS} is the degree of polymerization of the faster diffusing PS molecules. Since the tracer diffusion coefficient D^* of d-PS dominates D, our results are in excellent agreement with the fast theory, and in strong disagreement with the slow theory, of mutual diffusion.

2. From the measured values of $D(T)$ and $D^*(T)$ at $\phi = 0.55$, the Flory–Huggins interaction parameter χ is found to be $\chi = 0.112 - 62/T$. At a low diffusion temperature T, $D(T)$ is enhanced relative to the values of D^*; at high enough T's, however, a thermodynamic slowing down of D is observed as χ becomes positive.

3. An enhanced mutual diffusion coefficient $D(\phi)$ was observed at intermediate compositions of d-PS/PXE. Using calculated values of $\chi(T)$ for the $\phi = 0.55$ blend and the measured values of $D^*(\phi)$ for d-PS and d-PXE, we can successfully predict $D(\phi)$ across the entire composition range suggesting that the composition dependence of χ is weak.

Appendix

Temperature Dependence of the Tracer Diffusion Coefficient: Equation 10 was derived by noting that both T/D^* and the zero-shear rate viscosity η_0 are directly proportional to the monomeric friction coefficient ζ_0.[43,44] Since ζ_0 reflects the majority of the temperature dependence of D^*/T and η_0^{-1},[29] we can write

$$\log (\eta_0) = -\log (D^*/T) + \log (\text{constant}) \qquad (A1)$$

Since $\eta_0(T)$ is also given by the Vogel–Fulcher relationship,[45] we have

$$\log (\eta_0) = -\log (D^*/T) + \log (\text{constant}) = A + \frac{B}{(T - T_\infty)} \qquad (A2)$$

where A, B, and T_∞ are empirical parameters. Writing a similar expression for $\eta_{ref}(T_{ref})$ and then subtracting this from eq A2, one finds that

$$-\log\left(\frac{D^* T_{ref}}{D^*_{ref} T}\right) = \frac{B}{(T - T_\infty)} - \frac{B}{(T_{ref} - T_\infty)} \qquad (A3)$$

or

$$\log\left(\frac{D^* T_{ref}}{T}\right) = A' - \frac{B}{(T - T_\infty)} \qquad (A4)$$

where $A' = [B/(T_\infty - T_{ref})] - \log D_{ref}$.

Acknowledgment. This work was supported by the Division of Materials Research, NSF Polymers program, and we benefitted from the use of the facilities of the Cornell Materials Science Center which is funded by the Division of Materials Research—Materials Research Laboratory program of the NSF. We especially thank J. W. Mayer for his encouragement and appreciate useful discussions and correspondence with H. Sillescu, K. Binder, J. H. Wendorff, G. Fytas, P.-G. de Gennes, F. Brochard-Wyart, J. Klein, R. A. L. Jones, and A. M. Donald.

Registry No. PS, 9003-53-6; PXE (SRU), 39342-70-6; PXE (homopolymer), 39342-71-7.

Supplementary Material Available: Tables of data for Figures 5–9 (5 pages). Ordering information is given on any current masthead page.

References and Notes

(1) Composto, R. J.; Mayer, J. W.; Kramer, E. J.; White, D. M. *Phys. Rev. Lett.* **1986**, *57*, 1312.

(2) Brochard, F.; Jouffroy, J.; Levinson, P. *Macromolecules* **1983**, *16*, 1638.

(3) Binder, K. *J. Chem. Phys.* **1983**, *79*, 6387.

(4) Kramer, E. J.; Green, P. F.; Palmstrøm, C. J. *Polymer* **1984**, *25*, 473.

(5) Sillescu, H. *Makromol. Chem., Rapid Commun.* **1984**, *5*, 519.

(6) Sillescu, H. *Makromol. Chem., Rapid Commun.* **1987**, *8*, 393.

(7) Composto, R. J.; Kramer, E. J.; White, D. M. *Nature (London)* **1987**, *328*, 1980.

(8) Jones, R. A. L.; Klein, J.; Donald, A. M. *Nature (London)* **1986**, *321*, 161.

(9) Jones, R. A. L.; Rocca, S. A.; Donald, A. M.; Klein, J., unpublished results.

(10) Gilmore, P. T.; Falabella, R. Laurence, R. L. *Macromolecules* **1980**, *13*, 880.

(11) (a) Garabella, R. W.; Wendorff, J. H. *Makromol. Chem., Rapid Commun.* **1986**, *7*, 591. (b) Garabella, R. W.; Wendorff, J. H. submitted for publication in *Macromolecules.*

(12) Wu, S.; Chuang, H. K.; Han, C. D. *J. Polym. Sci., Polym. Phys. Ed.* **1986**, *24*, 143.

(13) (a) Murschall, U.; Fischer, E. W.; Herkt-Maetzky, Ch.; Fytas, G. J. *J. Polym. Sci., Polym. Lett.* **1986**, *24*, 191. (b) Brereton, M. G., Fischer, E. W.; Fytas, G.; Murschall, U. submitted for publication in *J. Chem. Phys.*

(14) de Gennes, P.-G. *J. Chem. Phys.* **1980**, *72*, 4756.

(15) Flory, P. J. *Principles of Polymer Chemistry*; Cornell University Press: Ithaca, NY, 1953; p 507.

(16) Shewmon, P. G. *Diffusion in Solids*; McGraw-Hill: New York, 1963.

(17) Crank, J. *The Mathematics of Diffusion*, 2nd ed.; Oxford University Press: Oxford, 1975.

(18) For a review of tracer diffusion, see: Tirrell, M. *Rubber Chem. Technol.* **1984**, *57*, 523.

(19) Green, P. F.; Palmstrøm, C. J.; Mayer, J. W.; Kramer, E. J. *Macromolecules* **1985**, *18*, 501.

(20) Brochard, F.; de Gennes, P.-G. *Europhys. Lett.* **1986**, *1*, 221.

(21) Brochard-Wyart, F. *C. R. Acad. Sci., Ser. 2* **1987**, *305*, 657.

(22) It is possible for blends which have a small positive χ to be compatible. See: Bates, F. S.; Wignall, G. D.; Koehler, W. C. *Phys. Rev. Lett.* **1985**, *55*, 2425. Bates, F. S.; Wignall, G. D. *Macromolecules* **1986**, *19*, 934.

(23) Doyle, B. L.; Peercy, P. S. *Appl. Phys. Lett.* **1979**, *34*, 822.

(24) Turos, A.; Meyer, O. *Nucl. Instrum. Methods* **1984**, *149*, 92.

(25) Green, P. F.; Mills, P. J.; Palmstrøm, C. J.; Mayer, J. W.; Kramer, E. J. *Phys. Rev. Lett.* **1984**, *53*, 2145.

(26) Mills, P. J.; Green, P. F.; Palmstrøm, C. J.; Mayer, J. W.; Kramer, E. J. *Appl. Phys. Lett.* **1984**, *45*, 957.

(27) Composto, R. J. Ph.D. Thesis, Cornell University, 1987.

(28) We measured D^*_{PXE} for $N_{PXE} = 225$ and 384 and then scaled these D^*'s (i.e., from reptation $D^* \propto N^{-2}$) so as to find the D^*_{PXE} for $N_{PXE} = 292$.

(29) Green, P. F.; Kramer, E. J. *J. Mater. Res.* **1986**, *1*, 202.

(30) Since the molar volumes of the PS and PXE monomers differ slightly, it is necessary to chose a reference volume of a cell on the quasi-lattice and to adjust the degree of polymerization accordingly. As our reference volume we have chosen the volume of a PS monomer at the particular temperature. The N_{PXE} was multiplied by the ratio of the molar volumes of PXE and PS by using the volume versus temperature data of ref 40.

(31) Green, P. F.; Doyle, B. L. *Phys. Rev. Lett.* **1986**, *57*, 2407.

(32) Shibayama, M.; Yang, H.; Stein, R. S.; Han, C. C. *Macromolecules* **1985**, *18*, 2179.

(33) Jelenic, J.; Kirste, R. G.; Oberthur, R. C.; Schmitt-Strecker, S.; Schmitt, B. J. *Macromol. Chem.* **1984**, *185*, 129.

(34) Maconnachie, A.; Kambour, R. P.; White, D. M.; Rostami, S.; Walsh, D. J. *Macromolecules* **1984**, *17*, 129.

(35) Wignall, G. D.; Child, H. R.; Aravena, F. Li *Polymer* **1980**, *21*, 131.

(36) Maconnachie, A.; Kambour, R. P.; Bopp, R. C. *Polymer* **1984**, *25*, 357.

(37) Kramer, E. J.; Sillescu, H., unpublished results.

(38) Yang, H.; Shibayama, M.; Stein, R. S.; Shimizu, N.; Hashimoto, T. *Macromolecules* **1986**, *19*, 1667.

(39) Athkin, E. L.; Kleintjen, L. A.; Koningsveld, R.; Fetters, L. J. *Polym. Bull. (Berlin)* **1982**, *8*, 347.

(40) Zoller, P.; Hoehn, H. H. *J. Polym. Sci., Polym. Phys. Ed.* **1982**, *20*, 1385.

(41) Jordan, E. A.; Ball, R. C.; Donald, A. M.; Fetters, L. J.; Jones, R. A. L.; Klein, J. *Macromolecules*, in press.

(42) Cohen, C., private communication.

(43) Graessley, W. W. *Adv. Polym. Sci.* **1982**, *47*, 67.

(44) Berry, G. C.; Fox, T. G. *Adv. Polym. Sci.* **1968**, *5*, 261.

(45) Ferry, J. D. *Viscoelastic Properties of Polymers*, 3rd ed.; Wiley: New York, 1981; Chapter 11.